Distributed Antenna Aided Twin-Layer Femto-and Macro-Cell Networks Relying on Fractional Frequency-Reuse

Jie Zhang†*, Fan Jin*, Rong Zhang*, Guangjun Li† and Lajos Hanzo*
†School of Comm. and Info. Engineering, UESTC, China.
∗School of ECS., Univ. of Southampton, SO17 1BJ, UK.
Email: {jz4,fj1g10,rz,lh}@ecs.soton.ac.uk, http://www-mobile.ecs.soton.ac.uk

***Abstract*— Distributed Antenna Systems (DAS) and femtocells are capable of improving the attainable performance in the cell-edge area and in indoor residential areas, respectively. In order to achieve a high spectral efficiency, both the Distributed Antenna Elements (DAEs) and Femtocell Base Stations (FBSs) may have to reuse the spectrum of the macrocellular network. As a result, the performance of both outdoor macrocell users and indoor femtocell users suffers from Co-Channel Interference (CCI). Hence in this paper, heterogenous cellular networks are investigated, where the DAS-aided macrocells and femtocells co-exist within the same area. The outage probability is derived and the network is optimised for minimising the outage probability. Our analysis demonstrates that surprisingly, the Unity Frequency Reuse (UFR) based macrocellular system can be optimised in isolation, without considering the impact of femtocells. We found that the macrocells relying on hard-FFR as well as on soft-FFR tend to migrate to several small cells, illuminated by the DAEs, when the density of femtocells becomes high.**

I. Introduction

Heterogeneous Networks (HetNet) have become an essential part of the contemporary wireless landscape, since they are capable of achieving an improved coverage and power efficiency. A paradigm shift is taking place, indicating a trend, moving away from traditional high-power tower-mounted base stations (BS) towards heterogeneous low-power infrastructure elements [1]. This evolution relies on a diverse combination of techniques.

Most current literature on HetNets is focused on a simple conglomerate of heterogeneous network elements. By contrast, in this paper we consider two specific aspects of HetNets. Firstly, we consider a twin-layer network constituted by FemtoCells (FC) overlaid on Distributed Antenna System (DAS) aided MacroCells (MC) from a network-structural perspective. Secondly, we investigate three typical frequency planning arrangements of MCs, namely Unity Frequency Reuse (UFR), soft Fractional Frequency Reuse (soft-FFR) and hard Fractional Frequency Reuse (hard-FFR). Let us elaborate a little further on the rationale of these focal points.

The main limitation of cellular networks is the ubiquitous Co-Channel Interference (CCI) [2], which is particularly damaging in the cell-edge area of systems employing the radical UFR. A straightforward practical solution for avoiding the strong CCI is to allocate orthogonal frequency bands within adjacent cells and reuse them in a certain pattern by exploiting the pathloss-induced attenuation, leading to traditional Frequency Reuse (FR). A more sophisticated technique of exploiting the available frequency band is constituted by the FFR in its hard-FFR [3] and soft-FFR [4] variants, both of which improve the Area Spectral Efficiency (ASE) of classic FR, while maintaining a high Signal-to-Interference-Ratio (SIR) in the cell-edge area. To elaborate a little further, the philosophy of FFR is that each cell is divided into a Cell-Centre Region (CCR) having access to the cell-centre's frequency band F_c and the Cell-Edge Region (CER) having access to the cell-edge's frequency band F_e.

In contrast to classic frequency planning invoked for combating the CCI, the DAS philosophy aims for providing an increased capacity, as its main design objective. Firstly, this is because the DAS may provide a shorter link between the Distributed Antenna Elements (DAEs) and the Mobile Station (MS) than that provided by the Macrocell Base Station (MBS), leading to a Reduced-Pathloss (RPL). Secondly, the DAS is capable of supporting several MSs within the same frequency band by exploiting their angular separation, leading to an angular *multiplexing gain*. Finally, when treating a DAS as a distributed Multi-User Multiple-Input and Multiple-Output (MU-MIMO) system, invoking advanced signal processing leads to both a macro-diversity gain and a multi-user gain[1]. As a result, in a FFR system, we may naturally opt for a DAS in the CER, which is capable of further improving both the ASE and the achievable SIR of the CER.

Having considered the above-mentioned outdoor cellular performance issues, the coverage and capacity problem may even be more serious in indoor scenarios. In order to meet the traffic demands of indoor mobile users, FCs have been invoked as a cost-effective way of balancing the traffic of the entire cellular system. FCs may be overlaid onto MCs, forming a hierarchical twin-layer network structure [5].

In order to support both the outdoor cellular users and indoor home users, operators may take advantage of the above three different approaches. Hence, we consider a DAS-aided twin-layer multi-cell network and investigate, whether these promising techniques may be beneficially amalgamated. In particular, a range of important issues arise, such as the interference aspects of the twin-layer network, the employment of DASs, the power allocation of DASs as well as their frequency partitioning. Our contributions are as follows

- *We invoke stochastic geometry [6], [7] for modelling the random distribution of FCs. The Outage Probability (OP) of outdoor MC users is derived in DAS-aided twin-layer networks. In contrast to [8], [9], the multicell interference is also considered.*
- *We study the impact of FCs on the existing DAS-aided MCs subject to different frequency planning strategies*

The financial support of the RC-UK under the auspices of the India-UK Advanced Technology Centre (IU-ATC) and that of the EPSRC under the China-UK science bridge as well as that of the EU's Concerto project is gratefully acknowledged.

[1]However, due to the length limitation of our paper, we will not treat the most advanced applications of DASs in this paper.

and optimise the DAS parameters, namely the power allocation between MBSs and DAEs as well as the FFR-related frequency partitioning factor in order to minimise the OP. This is achieved by improving the design approach of [10] by amalgamating it with a Quality of Service (QoS) constrained design[2].

The paper is organized as follows. In Section II, we describe our system model. Section III elaborates on the analysis of DAS-aided twin-layer networks and then the corresponding optimisation problems are presented in Section IV. Finally, our numerical results are provided in Section V and our conclusions are offered in Section VI.

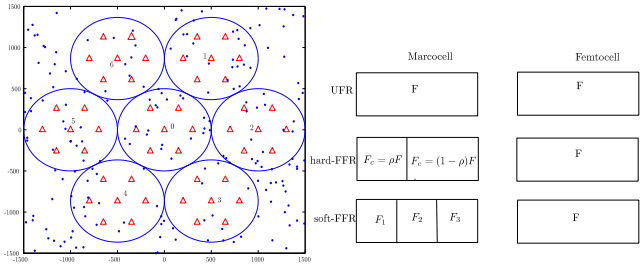

Fig. 1: The topology of the DAS-aided twin-layer cellular network and the frequency reuse strategies.

II. System Model

A. Topology Model

The topology of our DAS-aided cellular network is illustrated in Fig. 1, where the over-sailing MCs are overlaid on top of the FCs and N_a DAEs are employed in the CER of each MC, which are denoted by the triangles shown in Fig. 1.

For analytical convenience, we model the MCs as circles with radii of R_m, where the central target MBS B_0^m is surrounded by six adjacent tier-one MBSs $B_i^m, i \in 1, 2, \cdots, 6$. Within the ith MBS B_i^m, $N_a = 6$ DAEs denoted as $B_{i,j}^a, i \in 0, 1, \cdots, 6; j \in, 1, \cdots, N_a$ are arranged symmetrically in the CER having radii of r_d, which are far from the MBS B_i^m. Observe furthermore from Fig. 1 that the FBSs $B_n^f, n \in \mathbb{N}$ are represented by the small circles within the area, which are randomly distributed, obeying a homogeneous Spatial Poisson Point Process (SPPP) according to an area-density of λ. Here, we denote the overall FBS set by Ψ, which is overlaid onto the DAS-aided MC network. The coverage area of each FBS is assumed to be a circle having a radius of R_f. In addition to the above BS configuration, we assume both the Outdoor MC Users (OMUs) and the Indoor FC Users (IFUs) to be independently and uniformly distributed in their coverage area. Furthermore, the MBSs and DAEs will transmit their signals at their maximum power allowance of P_b and P_a, respectively, while obeying the total transmit power constraint of $P_b + N_a P_a = P_t$, with P_t denoting the total transmit power available for each MC. Similarly, the FBSs will transmit their signals at their maximum power allowance of P_f.

[2]Given the length limitation of our paper, we consider the impact of FCs imposed on DAS-aided MCs, and will consider a holistically optimised solution in our future research.

In this paper, we consider three different FR strategies, namely UFR, hard-FFR and soft-FFR scenarios. For the UFR scenario, the total available bandwidth F is used by both the MBS and by each DAE, where the OMUs are served either by the MBS or by the nearest DAE. In a hard-FFR scenario, the total available bandwidth F is partitioned into four orthogonal frequency bands, namely F_c, F_1, F_2 and F_3, obeying $F = F_c + F_1 + F_2 + F_3$, where we assume that $F_c = \rho F$ and $F_e = F_1 + F_2 + F_3 = (1-\rho)F$. Furthermore, F_c represents the frequency bands available for the CCR, while $F_i, i \in 1, 2, 3$ represents the frequency bands available for the CER in one of the three adjacent MCs. When considering the soft-FFR strategy, the total available bandwidth F is equally divided into three orthogonal frequency bands according to $F = F_1 + F_2 + F_3$, where one of the frequency bands $F_i, i \in 1, 2, 3$ is used in the CER, which is orthogonal to the neighbouring CER of the adjacent cells. On the other hand, the remaining two-thirds of the frequency band is reserved for the CCR.

B. Channel Model

In this paper, we assume that the DL channel is subject to uncorrelated Rayleigh fading obeying a unity average power constraint, as well as to wall-penetration loss and path-loss. For analytical simplicity, we considered a CCI-limited scenario and hence neglected the thermal noise in this paper. However, the consideration of the noise is straightforward. We let d_i and $d_{i,j}$ denote the distance from a user to the ith MBS B_i^m and to the jth DAE in the ith MC $B_{i,j}^a$, respectively, while d_{f_n} represents the distance between the user and the nth FBS B_n^f. The DL propagation loss may be categorised as:

1) *MBS / DAE to OMU:* The DL pathloss between the MBS B_i^m / the DAE $B_{i,j}^a$ and an OMU is modeled as $L_{m,dB} = A_O + 10\alpha_1 \log_{10}(d_i)$ and $L_{m,dB} = A_O + 10\alpha_1 \log_{10}(d_{i,j})$ in dB, while α_1 denotes the outdoor pathloss exponent and $A_O = 33.26 \log_{10}(f_c) - 79.86$ is constant in dB that depends on the carrier frequency f_c in MHz.
2) *FBS to OMU:* The DL pathloss between the FBS B_n^f and an OMU is modeled as $L_{m,f,dB} = A_O + 10\alpha_1 \log_{10}(d_{f_n}) + W$, where W denotes the wall-penetration loss in dB.

III. Analysis of DAS-aided Twin-layer Networks

In this section, the OP of DAS-aided twin-layer cellular networks will be derived, where an outage occurs when the instantaneous received SIR γ of a transmission falls below a predefined threshold of γ_{th}.

A. Outage probability of OMU within UFR scenario

The OMUs roaming in the CCR of the home MC B_0^m suffer from CCI imposed by the DAEs $B_{i,j}^a$, by six tier-one MBSs $B_i^m, i \neq 0$, as well as by the interfering FBSs B_{f_n}. As a result, the associated SIR γ_u of OMU u in the CCR, which is located at a radius of r_u and at an angle of θ_u, but sufficiently far away from its home MBS B_0^m, is given by:

$$\gamma_u = \frac{\xi_0 h_0}{\sum_{i \neq 0} \xi_i h_i + \sum_i \sum_j \xi_{i,j} h_{i,j} + \sum_n K d_{f_n}^{-\alpha_1} g_n}, \quad (1)$$

where h_i, $h_{i,j}$ and g_n denote the negative exponentially decaying channel gain of unity mean with respect to (wrt) the MBS B_i^m, the DAE $B_{i,j}^a$ as well as the FBS B_n^f, respectively, while $K = \frac{P_f}{A_O W}$. Furthermore, $\xi_i = \frac{P_b}{A_O} d_i^{-\alpha_1}$ and $\xi_{i,j} = \frac{P_a}{A_O} d_{i,j}^{-\alpha_1}$ represent the average power at the OMU u received from the MBS B_i^m and from the DAE $B_{i,j}^a$, respectively.

When the OMUs are located at the CER, they will be served by the DAE having the highest average received power $\xi_{0,k}$. Then the received SIR γ_u of OMU having a radius of r_u and an angle of θ_u may be written as

$$\gamma_u = \frac{\xi_{0,k} h_{0,k}}{\sum_i \xi_i h_i + \sum \sum_{i,j \in \Phi} \xi_{i,j} h_{i,j} + \sum_n K d_{f_n}^{-\alpha_1} g_n}, \quad (2)$$

where Φ denotes all the DAEs set $B_{i,j}^a, i \in 0, 1, \cdots, 6, j \in 0, 1, \cdots, N_a$ excluding the serving DAE $B_{0,k}^a$.

In the DAS-aided twin-layer cellular network associated with UFR, the OP of OMUs is formulated in Lemma 1.

Lemma 1: When an OMU u located at a radius of r_u and an angle of θ_u, but far from its serving MBS B_0^m in a DAS-aided twin-layer cellular network associated with UFR, the OP $\mathcal{O}_u(\gamma_{th}|r_u, \theta_u) = P(\gamma_u \leq \gamma_{th})$ associated with the SIR threshold of γ_{th} may be written as

$$\mathcal{O}_u(\gamma_{th}|r_u, \theta_u) = \begin{cases} 1 - \Xi_{\xi_0} \prod_{i \neq 0} \Delta_{\xi_i, \xi_0} \prod_i \prod_j \Delta_{\xi_{i,j}, \xi_0} & u \in CCR, \\ 1 - \Xi_{\xi_{0,k}} \prod_i \Delta_{\xi_i, \xi_{0,k}} \prod \prod_{i,j \in \Phi} \Delta_{\xi_{i,j}, \xi_{0,k}} & u \in CER, \end{cases}$$

where we have

$$\Xi_x = \exp[-\pi \lambda C_{\alpha_1} K^{\frac{2}{\alpha_1}} x^{-\frac{2}{\alpha_1}} \gamma_{th}^{\frac{2}{\alpha_1}}], \quad (3)$$

$$\Delta_{a,b} = (1 + \frac{a}{b} \gamma_{th})^{-1}, \quad (4)$$

with $C_{\alpha_1} = \int_0^\infty \frac{1}{1 + s^{\frac{\alpha_1}{2}}} ds$.

Proof: See Appendix I. ■

The OMUs are typically assumed to be independently and uniformly distributed within the coverage area. The probability of the OMU u having a radius of r and an angle of θ, but far from its home MBS is given by

$$p(r_u = r, \theta_u = \theta) = \frac{r}{\pi R_m^2}. \quad (5)$$

As a result, the spatially averaged OP $\mathcal{O}_m$ of OMUs may be written as

$$\mathcal{O}_m(\gamma_{th}) = \int_0^{R_m} \int_0^{2\pi} \frac{r}{\pi R_m^2} \mathcal{O}_u(\gamma_{th}|r, \theta) dr d\theta. \quad (6)$$

B. Outage probability of OMU within hard-FFR scenario

In a hard-FFR scenario, the OMUs roaming in the CCR receive no CCI from the DAEs any more, hence the received SIR γ_u of the uth OMU having a radius of r_u and an angle of θ_u, but far from its home MBS may be expressed as

$$\gamma_u = \frac{\xi_0 h_0}{\sum_{i \neq 0} \xi_i h_i + \sum_n K d_{f_n}^{-\alpha_1} g_n}. \quad (7)$$

When the OMU is far from the home MBS and located in the CER, it will be served by the DAE having the highest received power $\xi_{0,k}$. The OMU may suffer from strong CCI imposed both by other DAEs within the same MC as well as by the interfering FBSs, and the corresponding SIR γ_u may be written as

$$\gamma_u = \frac{\xi_{0,k} h_{0,k}}{\sum_{j \neq k} \xi_{0,j} h_{0,j} + \sum_n K d_{f_n}^{-\alpha_1} g_n}. \quad (8)$$

Following a similar derivation to that of Lemma 1, the OP of OMUs operating in a hard-FFR scenario is given by Lemma 2.

Lemma 2: In DAS-aided twin-layer cellular networks associated with a hard-FFR frequency reuse pattern, the OP $\mathcal{O}_u(\gamma_{th}|r_u, \theta_u)$ of OMUs located at a radius of r_u and an angle of θ_u, but far from their home MBS may be written as

$$\mathcal{O}_u(\gamma_{th}|r_u, \theta_u) = \begin{cases} 1 - \Xi_{\xi_0} \prod_{i \neq 0} \Delta_{\xi_i, \xi_0} & u \in CCR, \\ 1 - \Xi_{\xi_{0,k}} \prod_{j \neq k} \Delta_{\xi_{0,j}, \xi_{0,k}} & u \in CER. \end{cases}$$

By exploiting the assumption that the OMUs are independently and uniformly distributed in the coverage area, the spatially averaged OP $\mathcal{O}_m(\gamma_{th})$ of OMUs may be written as

$$\mathcal{O}_m(\gamma_{th}) = \int_0^{R_m} \int_0^{2\pi} \frac{r}{\pi R_m^2} \mathcal{O}_u(\gamma_{th}|r, \theta) dr d\theta. \quad (9)$$

C. Outage probability of OMU within soft-FFR scenario

In a soft-FFR frequency reuse pattern, the OMUs roaming in the CCR suffer from no CCI due to the DAEs within the same MC any more in a soft-FFR scenario, while both the MBSs and DAEs of tier-one MCs impose CCI on the CCR's OMUs. As a result, the OP of OMUs in the CCR becomes worse than that of the hard-FFR scenario and the received SIR γ_u of the OMU u at the radius of r_u and angle of θ_u, but far from its anchor MBS may be expressed as

$$\gamma_u = \frac{\xi_0 h_0}{\sum_{i \neq 0} \xi_i h_i + \sum_{i \neq 0} \sum_j \xi_{i,j} h_{i,j} + \sum_n K d_{f_n}^{-\alpha_1} g_n}. \quad (10)$$

When the OMU is roaming in the CER, no CCI will be imposed by its anchor MBS, while its received SIR γ_u depends on the CCI emanating both from the tier-one MBSs as well as from the interfering FBSs using the same frequency band. The instantaneous received SIR may be written as

$$\gamma_u = \frac{\xi_{0,k} h_{0,k}}{\sum_{i \neq 0} \xi_i h_i + \sum_n K d_{f_n}^{-\alpha_1} g_n}. \quad (11)$$

Lemma 3: In DAS-aided twin-layer cellular networks associated with soft-FFR, the OP of OMU $\mathcal{O}_u(\gamma_{th}|r_u, \theta_u)$ may be written as

$$\mathcal{O}_u(\gamma_{th}|r_u, \theta_u) = \begin{cases} 1 - \Xi_{\xi_0} \prod_{i \neq 0} \Delta_{\xi_i, \xi_0} \prod_{i \neq 0} \prod_j \Delta_{\xi_{i,j}, \xi_0} & u \in CCR, \\ 1 - \Xi_{\xi_{0,k}} \prod_{i \neq 0} \Delta_{\xi_i, \xi_{0,k}} & u \in CER. \end{cases}$$

Similarly, the spatially averaged OP $\mathcal{O}_m(\gamma_{th})$ of OMUs may be written as

$$\mathcal{O}_m(\gamma_{th}) = \int_0^{R_m} \int_0^{2\pi} \frac{r}{\pi R_m^2} \mathcal{O}_u(\gamma_{th}|r, \theta) dr d\theta. \quad (12)$$

IV. Optimal Design of DAS-aided Twin-Layer Network

Having considered the above comprehensive lists of different DAS-aided options, let us now aim for optimising the corresponding system performance in terms of their spatially

averaged throughput and seamless coverage by invoking Genetic Algorithm (GA) aided optimisation.

We will focus our attention on the optimal design of the DAS-aided twin-layer system using UFR, hard-FFR and soft-FFR frequency reuse pattern. Specifically, we will optimise both the normalised radii r_d of the DAS and the power allocation factor $\mu = \frac{P_a}{P_b}$ for UFR and soft-FFR scenarios. Similarly, we will also optimise the normalised radii r_d of the DAS, the power allocation factor $\mu = \frac{P_a}{P_b}$ as well as the spectrum partitioning factor ρ of the hard-FFR scenario. The appropriate choice of these parameters is expected to minimise the spatially averaged OP $\mathcal{O}_m(\gamma_{th})$.

A. OP-based Design

In this paper, we present an OP-based design approach with the aim of minimising the spatially averaged OP $\mathcal{O}_m(\gamma_{th})$, where we stipulate the QoS requirement η, guaranteeing that the long-term spatially averaged CER throughput is at least a fraction η of the CCR throughput. Hence, the system parameters may be adjusted for trading the data-rates of the CCR MC users against those of the CER MC users. Given the predefined SIR threshold γ_{th}, the optimisation problem using this OP-based approach may be formulated as

$$\begin{aligned} \min \quad & \mathcal{O}_m(\gamma_{th}, r_d, \mu) = \int_0^{R_m} \int_0^{2\pi} \frac{r}{\pi R_m^2} \mathcal{O}_m(\gamma_{th}|r,\theta) dr d\theta \\ \text{s.t.} \quad & \frac{\rho_o N_a T_{m_2}(r_d,\mu)}{\rho_i T_{m_1}(r_d,\mu)} \geq \eta \\ & P_b + N_a P_a = P_t, \end{aligned} \tag{13}$$

where T_{m_1} and T_{m_2} denote the spatially averaged throughput within the CCR and the CER of the MC, respectively. Furthermore, ρ_o and ρ_i denote the normalised available frequency bands within the CER and within the CCR, respectively. More specifically, the normalised frequency bands available satisfy $\rho_o = \rho_i = 1$ within the UFR scenario and $\rho_o = \frac{1}{3}$ and $\rho_i = \frac{2}{3}$ within the soft-FFR scenario, while ρ_o and ρ_i are the function of the frequency partitioning factor ρ of $\rho_o = \frac{1-\rho}{3}$ and of $\rho_i = \rho$ within the hard-FFR scenario.

B. Optimisation tool

Since no closed-form equations have been found for the OP $\mathcal{O}_m(\gamma_{th}, r_d, \mu)$ and for the MC throughput $T_{m_i}(r_d, \mu), i \in 1, 2$, we solve the optimisation problems of Eq. (13) using the classic GA optimisation method [11], where $T_{m_1}(r_d, \mu)$ and $T_{m_2}(r_d, \mu)$ will be numerically evaluated with the aid of Matlab tools due to the fact that the three-fold integration is extremely time-consuming. The GA constitutes an attractive global heuristic optimisation tool for search problems, which mimics the process of natural evolution. A random population P is created first, and the fitness of each individual candidate-solution is evaluated. Then a number of high-fitness individuals are selected from the current generation of the population in order to create off-springs with the aid of using the standard crossover and mutation operations. The newly formed generation of the population is then used in the next iteration of the algorithm, hence the GA process leads to the gradual evolution of the population to better solutions of the optimisation problem.

TABLE I: Notations and System parameters

Symbol	Description	Value
f_c	Carrier frequency	2 GHz
D	Inter-Cell Distance	1000 m
R_f	Radius of the Femtocell	20 m
$A_{O,dB}$	Fixed outdoor pathloss	$33.26 \log_{10}(f_c) - 79.86$ dB
α_1	Outdoor pathloss exponent	4
W_{dB}	Wall penetration loss	5 dB
$P_{m,dB}$	MBS transmit power	46 dBm
$P_{f,dB}$	FBS transmit power	13 dBm

V. Performance Evaluation

In this section, we will evaluate the performance of DAS-aided twin-layer cellular networks using our UFR, hard-FFR and soft-FFR strategies. The CDF of the received SIR of OMUs is verified first, which is followed by the results of our optimal design. Our system parameters are summarised in Table I.

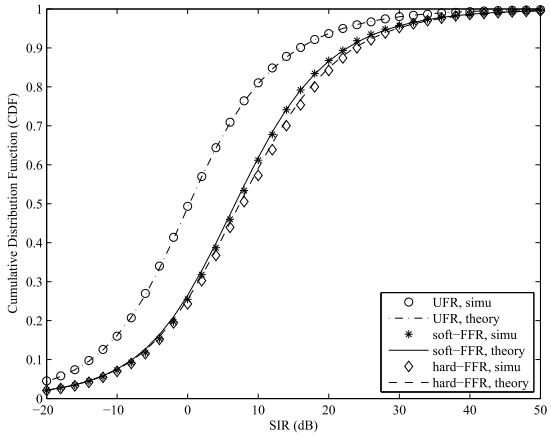

Fig. 2: The CDF of the received SIR, when the number of femtocells within each macrocell is $N_f = 50$.

A. CDF of Spatially Received SIR

Fig. 2 illustrates the CDF of the spatially averaged received SIR γ within DAS-aided twin-layer cellular networks, where the FBSs are randomly distributed obeying a homogeneous SPPP according to an area-density of $\lambda = \frac{N_f}{\pi R_m^2}$ with N_f denoting the number of FCs within each MC. Observe from Fig. 2 that the simulation results become slightly better than the theoretical results, because we only considered the CCI arriving from the interfering FBSs within a circle having a radius of R_m, but ignored the CCI imposed by the FBSs far away from the user considered in our simulations. It is clearly shown that as expected, the received SIR of the hard-FFR scenario is better than that of the soft-FFR and UFR scenario, which is due to the fact that no CCI is imposed either by the tier-one MBSs or by the DAEs within the tier-one MCs, while the received SIR of the UFR scenario becomes the worst amongst all frequency reuse patterns, as a result of the strong CCI within the same MC.

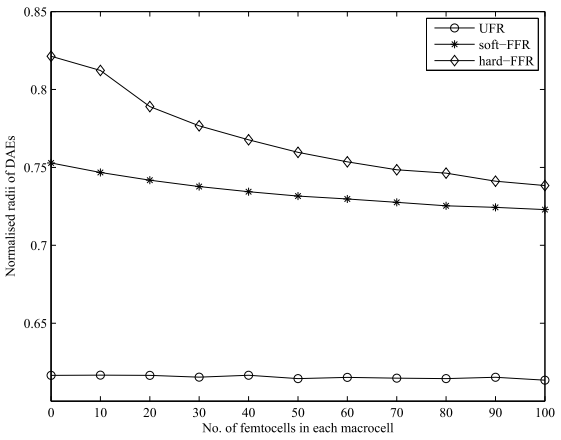

Fig. 3: The optimised normalised radii of DAS r_d in the OP-based design.

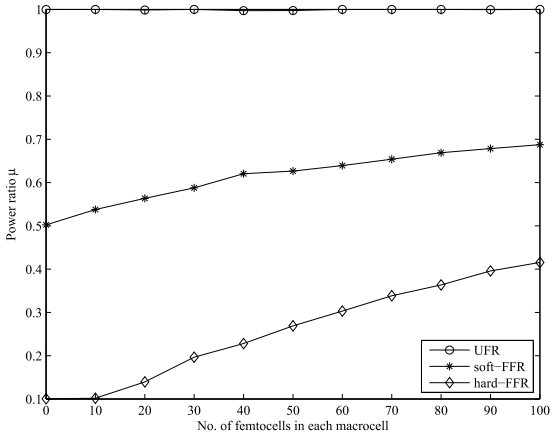

Fig. 4: The optimised power allocation μ in the OP-based design.

B. Optimised design for DAS-aided twin-layer cellular networks

In order to highlight the importance of optimal parameter design, we investigate the performance of the OP-based design of our DAS-aided twin-layer network, where a QoS constraint of $\eta = 0.2$ is considered. We also considered a static system configuration of $r_d = \frac{2}{3}$ and $\mu = 1.0$ as the benchmarker, which is referred to as *System 1 (S1)*.

Fig. 3 and Fig. 4 illustrate the optimised system configurations as a function of the number of FCs N_f in the UFR, hard-FFR and soft-FFR scenarios. Observe from both figures that the UFR scenario relies on the near-constant parameters of $r_d \approx 0.62$ and $\mu \approx 1$, which are independent of the number of FCs N_f. In other words, the system parameters of the UFR scenario can be configured separately, entirely without considering the impact of the interfering FCs. However, the optimised radius r_d of the DAS tends to decrease upon increasing the number of FCs for both the hard-FFR and soft-FFR scenario, which are sensitive to the density of the FCs. Furthermore, the optimised power allocation factor μ tends to increase, as the number of FCs N_f increases. In the CCR, the performance of both the hard-FFR and of the soft-FFR scenario becomes worse than that of the CER, when the density of FCs increases. As a result, the OMUs have to be handed over from the MBS to the DAEs of the CER of twin-layer networks in the presence of high-density interfering FCs, which may be viewed, as the MCs being split into several DAS-based small cells in order to maintain a low OP.

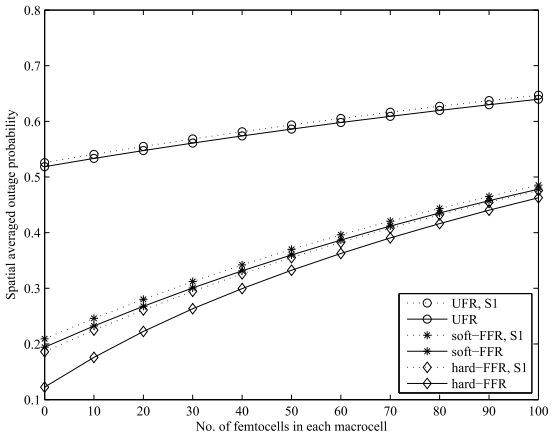

Fig. 5: The spatially averaged OP in the OP-based design, when the SIR threshold is $\gamma_{th} = 3dB$.

Fig. 5 compares the spatially averaged OP of S1 and of the GA-aided near-optimal networks, where the SIR threshold is set to $\gamma_{th} = 3dB$. It is clearly shown in Fig. 5 that as expected, the spatially averaged OP increases with the number of FCs within all scenarios considered. More specifically, the OP $\mathcal{O}_m(\gamma_{th})$ of the UFR scenario is significantly higher than that of both the hard-FFR and soft-FFR scenario, duo to the fact that the CCI imposed on the OMUs of the UFR scenario is significantly higher than in the other two scenarios. Furthermore, the OP of the hard-FFR scenario is lower than that of the soft-FFR, which is achieved at the cost of a reduced throughput. However, the OP of the hard-FFR increases more rapidly than that of soft-FFR and then becomes somewhat lower than that of the soft-FFR scenario, when the density of FCs λ is high. Fig. 5 also shows that the OP of the GA-based near-optimal networks always remains better than that of the benchmarker S1, especially for the low-density femtocellular hard-FFR scenario.

VI. Conclusions

In this paper, we have provided the analysis and the GA-based near-optimal design of DAS-aided twin-layer cellular networks associated with UFR, hard-FFR and soft-FFR scenarios, where the OP was derived. The GA-based near-optimal design of this twin-layer cellular system for the UFR, hard-FFR as well as soft-FFR scenarios has been investigated, with the goal of minimising the spatially averaged OP. We have found that the optimised design for the UFR scenario is independent of the density of the interfering FCs, suggesting

that the system can be optimised without considering the impact of the FCs. As for the hard-FFR and the soft-FFR scenario operating in the presence of high-density FCs, the optimised MC tends to migrate to smaller cells illuminated by the DAEs in order to maintain a low OP.

APPENDIX I
OUTAGE PROBABILITY WITHIN UFR SCENARIO

When UFR is considered, the received SIR γ_u of OMU u within the CCR is rewritten from Eq. (1) as

$$\gamma_u = \frac{h_0}{I_1 + I_2 + I_3}, \tag{14}$$

where we have $I_1 = \sum_{i\neq 0} \frac{\xi_i}{\xi_0} h_i$, $I_2 = \sum_i \sum_j \frac{\xi_{i,j}}{\xi_0} h_{i,j}$ and $I_3 = \sum_n \frac{K d_{f_n}^{-\alpha_1}}{\xi_0} g_n$. Duo to the fact that the interference terms I_1, I_2 and I_3 are independent of each other and the channel gain h_i is negative exponentially decaying, the OP $\mathcal{O}_u(\gamma_{th}|r_u, \theta_u)$ of the CCR's OMU at a radius of r_u and angle of θ_u may be written as

$$\begin{aligned}
\mathcal{O}_u(\gamma_{th}|r_u,\theta_u) &= 1 - P(\gamma_u \geq \gamma_{th}|r_u,\theta_u) \\
&= 1 - P[h_0 \geq \gamma_{th}(I_1+I_2+I_3)|r_u,\theta_u] \\
&= 1 - \exp[-\gamma_{th}(I_1+I_2+I_3)] \\
&= 1 - \exp(-\gamma_{th}I_1)\exp(-\gamma_{th}I_2)\exp(-\gamma_{th}I_3) \\
&= 1 - \mathcal{L}_{I_1}(\gamma_{th})\mathcal{L}_{I_2}(\gamma_{th})\mathcal{L}_{I_3}(\gamma_{th}),
\end{aligned} \tag{15}$$

where $\mathcal{L}_{I_1}$, $\mathcal{L}_{I_2}$ and $\mathcal{L}_{I_3}$ denote the Laplace transform of the random variable I_1, I_2 and I_3, respectively. The term I_1 is the linear sum of independent exponential distributed random variable h_i, the Laplace transform of $\mathcal{L}_{I_1}$ can be directly derived as

$$\begin{aligned}
\mathcal{L}_{I_1}(\gamma_{th}) &= E\Big[\exp(-\gamma_{th}\sum_{i\neq 0}\frac{\xi_i}{\xi_0}h_i)\Big] \\
&= \prod_{i\neq 0} E\Big[\exp(-\frac{\xi_i}{\xi_0}\gamma_{th}h_i)\Big] \\
&\overset{(a)}{=} \prod_{i\neq 0}(1+\frac{\xi_i}{\xi_0}\gamma_{th})^{-1},
\end{aligned} \tag{16}$$

where (a) follows the Laplace transform of exponential random variables. Similarly, the Laplace transform of the interference term I_2 may be written as

$$\mathcal{L}_{I_2}(\gamma_{th}) = \prod_i \prod_j (1+\frac{\xi_{i,j}}{\xi_0}\gamma_{th})^{-1}. \tag{17}$$

The Laplace transform of the sum of SPPP I_3 is given by

$$\begin{aligned}
\mathcal{L}_{I_3}(\gamma_{th}) &= E_{\Psi,g_n}\Big[\exp(-\sum_{n\in\Psi}\frac{K\gamma_{th}}{\xi_0}d_{f_n}^{-\alpha_1}g_n)\Big] \\
&= E_{\Psi,g_n}\Big[\prod_{n\in\Psi}\exp(-\frac{K\gamma_{th}}{\xi_0}d_{f_n}^{-\alpha_1}g_n)\Big] \\
&= E_{\Psi}\Big\{\prod_{n\in\Psi}E_{g_n}\Big[\exp(-\frac{K\gamma_{th}}{\xi_0}d_{f_n}^{-\alpha_1}g_n)\Big]\Big\} \\
&\overset{(b)}{=} E_{\Psi}\Big[\prod_{n\in\Psi}(1+\frac{K\gamma_{th}}{\xi_0}d_{f_n}^{-\alpha_1})^{-1}\Big] \\
&\overset{(c)}{=} \exp\Big[-2\pi\lambda\int_0^{\infty}(1-\frac{1}{1+\frac{K\gamma_{th}}{\xi_0}t^{-\alpha_1}})tdt\Big] \\
&= \exp\Big[-\pi\lambda C_{\alpha_1}(\frac{K\gamma_{th}}{\xi_0})^{\frac{2}{\alpha_1}}\Big],
\end{aligned} \tag{18}$$

where (b), again, follows the Laplace transform of exponential distributed variables and (c) follows from the Probability Generating Functional (PGFL) of the SPPP [6]. Substituting Eq. (16), Eq. (17) and Eq. (18) into Eq. (15), the OP of OMU within the CCR at a radius of r_u and angle of θ_u can be derived as

$$\mathcal{O}_u(\gamma_{th}|r_u,\theta_u) = 1 - \Xi_{\xi_0}\prod_{i\neq 0}\Delta_{\xi_i,\xi_0}\prod_i\prod_j\Xi_{\xi_{i,j},\xi_0}.$$

Following a similar derivation for the OP of the CCR's OMUs, the OP of the CER's OMU at a radius of r_u and angle of θ_u can be expressed as

$$\mathcal{O}_u(\gamma_{th}|r_u,\theta_u) = 1 - \Xi_{\xi_{0,k}}\prod_i\Delta_{\xi_i,\xi_{0,k}}\prod_{i,j\in\Phi}\Delta_{\xi_{i,j},\xi_{0,k}}.$$

REFERENCES

[1] A. Ghosh, N. Mangalvedhe, R. Ratasuk, B. Mondal, M. Cudak, E. Visotsky, T. A. Thomas, J. G. Andrews, P. Xia, H. S. Jo, H. S. Dhillon, and T. D. Novlan, "Heterogeneous cellular networks: From theory to practice," *IEEE Communications Magazine*, vol. 50, no. 6, pp. 54–64, Jun. 2012.

[2] R. Zhang and L. Hanzo, "Wireless cellular networks," *IEEE Vehicular Technology Magazine*, vol. 5, no. 4, pp. 31–39, Dec. 2010.

[3] G. Boudreau, J. Panicker, N. Guo, R. Wang, and S. Vrzic, "Interference coordination and cancellation for 4G networks," *IEEE Communications Magazine*, vol. 47, no. 4, pp. 74–81, Apr. 2009.

[4] T. D. Novlan, R. K. Ganti, A. Ghosh, and J. G. Andrews, "Analytical evaluation of fractional frequency reuse for OFDMA cellular networks," *IEEE Transactions on Wireless Communications*, vol. 10, no. 12, pp. 4294–4305, Dec. 2011.

[5] V. Chandrasekhar and J. G. Andrews, "Femtocell networks: A survey," *IEEE Communications Magazine*, vol. 46, pp. 59–67, Sep. 2008.

[6] M. Haenggi, J. G. Andrews, F. Baccelli, O. Dousse, and M. Franceschetti, "Stochastic geometry and random graphs for the analysis and design of wireless networks," *IEEE Journal on Selected Areas in Communications*, vol. 27, no. 7, pp. 1029–1046, Sep. 2009.

[7] F. Baccelli, B. Blaszczyszyn, and P. Muhlethaler, "Stochastic analysis of spatial and opportunistic aloha," *IEEE Journal on Selected Areas in Communications*, vol. 27, no. 7, pp. 1105–1119, Sep. 2009.

[8] V. Chandrasekhar and J. G. Andrews, "Uplink capacity and interference avoidance for two-tier femtocell networks," *IEEE Transactions on Wireless Communications*, vol. 8, pp. 3498–3509, July 2009.

[9] V. Chandrasekhar, M. Kountouris, and J. G. Andrews, "Coverage in multi-antenna two-tier networks," *IEEE Transactions on Wireless Communications*, vol. 8, no. 10, pp. 5314–5327, Oct. 2009.

[10] T. Novlan, J. G. Andrews, I. Sohn, and R. K. Ganti, "Comparison of fractional frequency reuse approaches in the OFDMA cellular downlink," in *Proc. IEEE GLOBECOM*, Jan. 2010, pp. 1–5.

[11] D. E. Goldberg, *Genetic Algorithms in Search, Optimization and Machine Learning*. Addison Wesley Publishing Company, 1989.